Fringe-Field Switching Transflective Displays

Y. J. Lim[1], M. O. Choi[1] and S. H. Lee[1]
[1]School of Advanced Material Engineering, Chonbuk National University, Chonju, Chonbuk, Korea
J. H. Song[2], Y. H. Jeong[2], H. Y. Kim[2], S. Y. Kim[2] and Y. J. Lim[2]
[2]SBU Development Center, BOE TFT-LCD SBU, Ichon-si, Gyeonggi-do, 467-701, Korea

Abstract

We have studied transflective liquid crystal displays (LCDs) associated with fringe-field switching (FFS) mode to achieve high image quality. In the past, several cell structures were used to fabricate transflective FFS liquid crystal displays. Their structures and characteristics are carefully examined to find their merits and cons. Further, optimization of cell parameters to achieve a single driving circuit is performed.

1. Objective and Background

Recently, transflective liquid crystal displays (LCDs) are being commercialized because they can be used in outdoor and indoor uses with relatively lower power consumption than that in transmissive display[1-3]. At present, the transflective displays are using twisted (TN) and homogenous cell (named ECB) with compensation film[4]. However, in both TN and ECB modes, the LC director tilts up in one direction along the vertical field direction so that the viewing angle is limited in the transmissive region. In fringe–field switching (FFS) mode, homogenously aligned LC reacts to applied voltage and rotates in one direction maintaining almost parallel to the substrate, thus, resulting high transmittance with wide viewing angle. Recently, many experiments and computer simulations on electro-optical characteristics of the transmissive[5-7] and reflective[8] FFS LCD were carried out. Further, many results on the FFS transflective displays such as homogenous cells with compensation film driven by fringe-electric field with dual cell gap[9], single cell gap with multi-driving circuit[10] as well as dual orientation[11] have been reported.

In the paper, their structures and characteristics are carefully examined to find their merits and cons. In each case, cell conditions were optimized to achieve single gap, single driving, single orientation and wide viewing angle transflective FFS liquid crystal display which is easy to fabricate.

2. Cell Structure of FFS Transflective Display and Their Characteristics

2.1 Dual gap Transflective FFS Display

Figure 1 shows calculated voltage-dependent light efficiency in the dual gap tansflective display using a LC with negative dielectric anisotropy (-LC). High light efficiency of 98% was achieved in both reflective and transmissive parts. Operation voltages for reflective and transmissive parts are 5.7 and 4.7V, respectively. The difference between reflectance and transmittance curves is originated because cell gap of reflective part is twice that of transmissive part. Moreover, light efficiency is reduced when cell gap is less than 2um in FFS mode with homogeneously aligned LC[12].

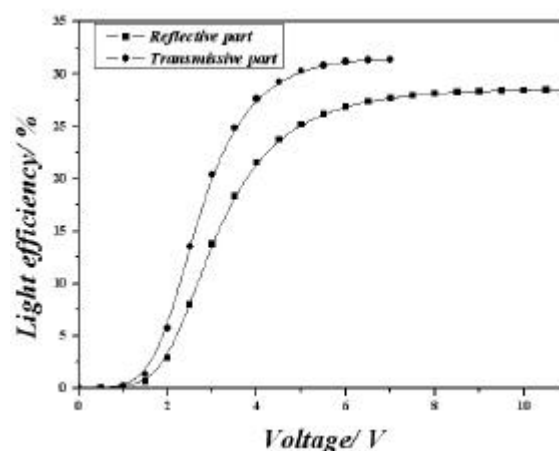Figure 1. Voltage-dependent light efficiency in the dual gap tansflective display.

Figure 2 shows iso-contrast curves in the T and R regions at an incident wavelength of 550nm. In this cell, the region ($R_{CR>5}$) in which the contrast ratio (CR) is larger than 5 exists at a polar angle of more than 50° in all directions in both the T and R regions.
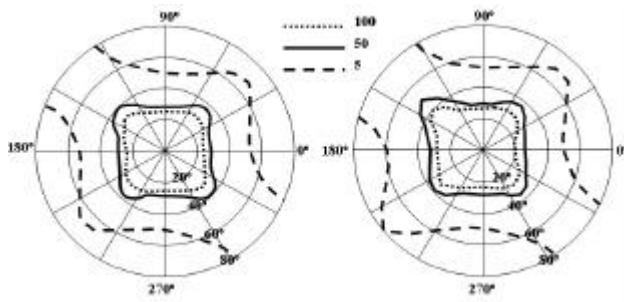
Figure 2. Iso-contrast contour at an incident wavelength of 550nm in the dual gap transflective display: (a) R-part, (b) T-part.

The merit of the dual gap transflective was high transmittance and wide viewing angle. The demerit of the dual gap transflective is high sensitivity of a dark state and dual cell gap, such that complex manufacturing process and unwanted LC alignment exists in the region between R- and T- parts.

2.2 Dual Orientation Transflective FFS Display

Figure 3 shows schematic cell structure of the dual orientation transflective display[11]. In the R region, the LC has a hybrid alignment while it has a homogeneous alignment in the T region. The LC on the bottom substrate has homogeneous alignment in both regions while the LC has dual alignment on the top substrate. As a result, the effective cell retardation value in the R region equals about half of the T region. Owing to this, a single gap transflective display is realized.
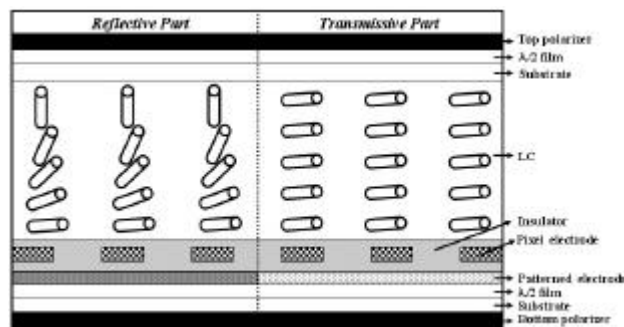

Figure 3. Schematic cell structure of the dual orientation transflective display.

Figure 4 (a) shows calculated voltage-dependent light efficiency in the dual orientation transflective

display when the wavelength of an incident light is 550nm, using the -LC. Here, the rubbing angle is 12° for both cases. In this cell, the R region has a slightly higher light efficiency than that in the T region since the optimal cell retardation value for maximal light efficiency is slightly. Figure 4 (b) shows calculated voltage-dependent light efficiency in the 20° rubbing angle at R-part and 5° rubbing angle at T-part when the wavelength of an incident light is 550nm, which reduces the difference between two curves. Further optimization of voltage-dependent T and R curves is required.
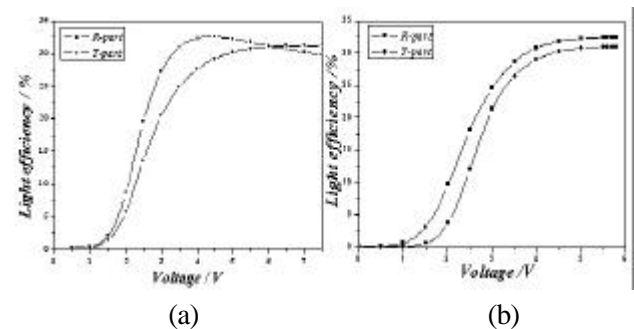

(a)   (b)

Figure 4. Voltage-dependent light efficiency in the dual orientation transflective display: (a) 12° rubbing angle at R-and T-part (b) 20° rubbing angle at R-part and 5° rubbing angle at T-part.

Figure 5 shows iso-contrast curves is the T and R regions at an incident wavelength of 550nm in the dual orientation transflective display. In this cell, the $R_{CR>5}$ exists at a polar angle of more than 50° in all directions in both the T and R regions.
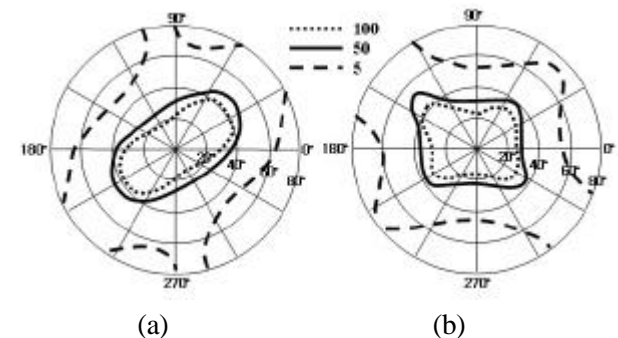

(a)   (b)

Figure 5. Iso-contrast contour at an incident wavelength of 550nm in the dual orientation transflective display: (a) R-part, (b) T-part.

The merit of the dual orientation transflective display is that the device can have a high single cell gap with wide viewing angle . The demerit of the dual orientation transflective is the formation of two domains, and high sensitivity of a dark state to cell retardation.

2.3 Single Cell Gap Transflective FFS Display

Figure 6 shows schematic cell structure of the single gap transflective display[13-14]. In the device, the pixel and counter electrodes exist only on the top substrate. The in-cell retarder with a quarter-wave plate($?/4$) exists above the patterned reflector. One compensation film with $?/4$ exists below bottom substrate. Two polarizers are crossed to each other and an optic axis of the LC coincides with one of the polarizer axes. With this structure, the existence of the in-cell retarder does not increase an operating voltage (V_{op}).
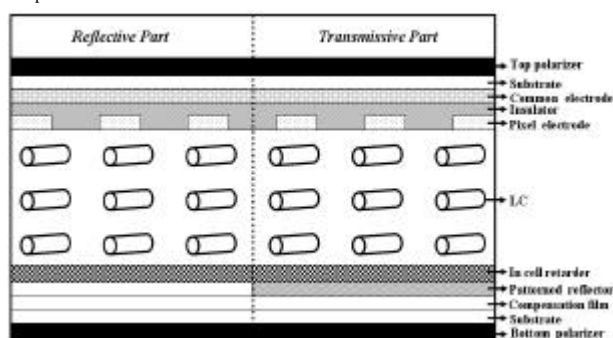

Figure 6. Schematic cell structure of the single gap transflective display.

Figure 7(a) shows voltage-dependent light efficiency in the single gap transflective display when using the -LC ($? e = -4.0$, rubbing angle 12°). Unfortunately, two curves do not coincide with each other. Figure 7(b) shows calculated voltage-dependent light efficiency in the 55° rubbing angle at R-part and 20° rubbing angle at T-part. This informs that a single driving circuit can control the applied voltage in both the reflective and transmissive region.

Figure 8 shows iso-contrast contour at an incident wavelength of 550nm in the single gap transflective display. In the *R* part, the $R_{CR>5}$ exists to about 50° of polar angle in all directions, except in certain diagonal directions, where it exists larger than 80° of polar angle. In the *T* area, the $R_{CR>5}$ was larger than 10 exists over 60° of polar angle in all directions.
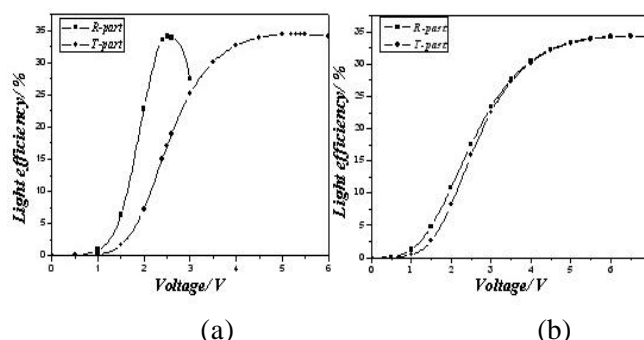

Figure 7. Voltage-dependent light efficiency in the single gap tansflective display when using negative LC: (a) 12° rubbing angle at R-and T-part (b) 55° rubbing angle at R-part and 20° rubbing angle at T-part.
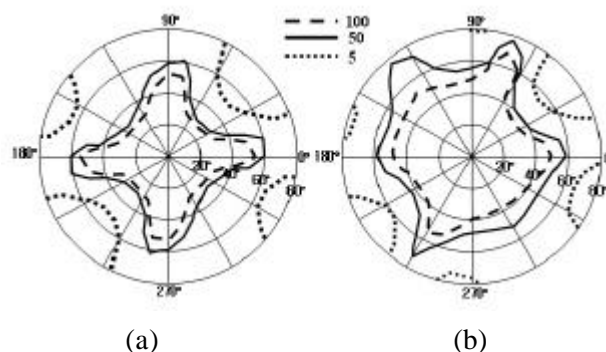

Figure 8. Iso-contrast contour at an incident wavelength of 550nm in the single gap transflective display using negative LC: (a) R-part, (b) T-part.

We also calculated a voltage-dependent reflectance and transmittance using the LC (+LC) with positive dielectric anisotropy ($? e = 7.4$, rubbing angle 80°), as shown in Figure 9(a). As indicated, two curves do not coincide with each other. Figure 9(b) shows calculated voltage-dependent light efficiency in the 45° rubbing angle at R-part and 80° rubbing angle at T-part when using the +LC. In this way, the difference in two curves is reduced.

Figure 10 shows iso-contrast contour at an incident wavelength of 550nm in the single gap transflective display using positive LC. In the *R* part, the $R_{CR>5}$ was larger than 5 exists to about 60° of polar angle in all directions, except in certain diagonal directions, where it exists larger than 80° of polar angle. In the *T* area, $R_{CR>5}$ exists over 70° of polar angle in all directions. In trasmissive and reflective parts, polar

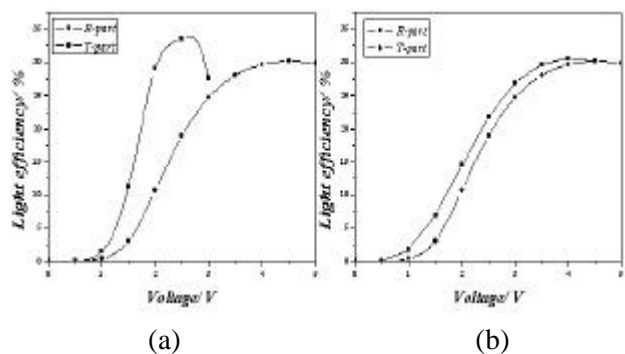angle is about 10° higher with the +LC than that with the -LC.

(a)   (b)

Figure 9. Voltage -dependent light efficiency in the single gap transflective display when using positive LC: (a) 80° rubbing angle at R-and T-part (b) 45° rubbing angle at R-part and 80° rubbing angle at T-part.
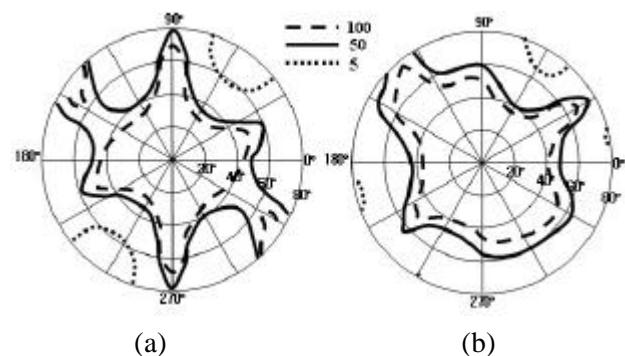

(a)   (b)

Figure 10. Iso-contrast contour at an incident wavelength of 550nm in the single gap tansflective display using positive LC: (a) R-part, (b) T-part.

The merit of the single gap transflective is that the dark state is not dependent on cell retardation value unlike other transflective cases with single cell gap and high image quality. However, the demerit is an extra process to coat the in-cell retarder.

3.   Impact
For the first time, we proposed single cell gap and single driving circuit with wide viewing angle transflective display using fringe-field. The device has

a potential to be applicable to small and medium-sized transflective display.

7.   References
[1] H-I. Baek, Y-B. Kim, K-S. Ha, D-G. Kim, S -B. Kwon, IDW'00, 41, 2000.

[2] Makoto Jisaki, Hidemasa Yamaguchi, IDW'01, 133, 2001.

[3] E. Yoda, T. Uesaka, T. Ogasawara, and T. Toyooka, SID' 02 Dig, 762, 2002.

[4] T. Uesaka, E. Yoda, T. Ogasawara and T. Toyooka, Proc. of the 9th IDW'02, p.417, 2002.

[5] S. H. Lee, S. L. Lee and H. Y. Kim, Appl. Phys. Lett., **73,** 2881, 1998.

[6] S. H. Lee, S. M. Lee, H. Y. Kim, J. M. Kim, S. H. Hong, Y. H. Jeong, C. H. Park, Y. J. Choi, J. Y. Lee, J. W. Koh, and H. S. park, SID'01, p. 484, 2001.

[7] S. H. Jung, H. Y. Kim, S. H. Song, J. H. Kim, S. H. Nam and S. H. Lee, Jpn. J. Appl. Phys, **43**, 1025, 2004.

[8] T. B. Jung, C. H. Park, H. Y. Kim, S. H. Hong, and S. H. Lee, Proc. of the 5th KLCC'02, p. 77, 2002.

[9] T. B. Jung, J. C. Kim and S. H. Lee, Jap. J. Appl. Phys. **42**, p. 464, 2003.

[10] J. H. Song, Y. J. Lim, and S. H. Lee, Submitted to Appl. Phys. Lett. 2005.

[11] Y. J. Lim, J. H. Song, Y. B. Kim, S. H. Lee, Jap. J. Appl. Phys. 43, 972, 2004.

[12] S. H. Lee, private communication.

[13] M. O. Choi, J. H. Song, Y. J. Lim, T. H. Kim and S. H. Lee, Submitted SID'05, 2005.

[14] Y. H. Jeong, H. Y. Kim, J. B. Park, M. S. Kim, G. H. Kim, S. M. Seen, D. H. Lim, S. Y. Kim, Y. J. Lim and S. H. Lee, Submitted SID'05, 2005.